Periodic Sampling Interval Repetitive Control and Its Application to Variable Spindle Speed Noncircular Turning Process

Reed D. Hanson[1]
Department of Mechanical and Industrial Engineering, University of Illinois at Urbana-Champaign, Urbana, IL 61801

Tsu-Chin Tsao
Mechanical and Aerospace Engineering Department, University of California, Los Angeles, Los Angeles, CA 90095-1597

This paper addresses discrete-time, repetitive control for linear, periodic, time-varying systems. A periodic, repetitive control design method based on gain scheduling is proposed and the necessary and sufficient condition for closed-loop stability is presented. Utilizing the special structure of the repetitive controller, an efficient method for evaluating the closed-loop stability is developed. The algorithm is applied to the control of a piezoelectric fast-tool stage for variable spindle speed noncircular turning process. The tool performs dynamic variable depth of cut machining to generate noncircular workpiece profiles while the spindle carrying the workpiece rotates at a variable speed to inhibit machining instability (chatter). Experimental machining results are presented that demonstrate the tracking performance of the period, time-varying controller design proposed, as well as the ability to increase machining stability using this approach.
[S0022-0434(00)02402-3]

1 Introduction

Repetitive control can achieve asymptotic tracking and disturbance rejection of periodic inputs, and it has been successfully applied to many areas. However, previous work in discrete-time, repetitive control has been restricted to time-invariant controller synthesis for systems sampled at a uniform sampling rate. When the application problem requires a periodic sampling rate, the sampled discrete-time model for a linear, time-invariant, continuous system becomes a periodically time-varying system.

The repetitive control with periodic sampling rate problem is motivated by two applications. First, periodic sampling rate is utilized to maintain a time-invariant tracking reference and/or disturbance model. One example is generating a periodic spindle speed profile in terms of spindle angle for radial runout compensation in milling (Tsao and Pong, [1,2]). Another example, which is the application example presented in this paper, is noncircular turning with periodically varying spindle speed to inhibit machining chatter instability. Second, in the digital tracking control of continuous, periodic signals with finite, real-time CPU processing power, inter-sample errors may be reduced by scheduling the sampling intervals with respect to the reference signal so that rapid sampling occurs when abrupt changes in the continuous reference signal take place. For example, in noncircular turning for camshafts, more points can be sampled at the cam lobe nose area and less points at the base circle area.

Repetitive control for linear, periodic systems has been previously studied by Omata et al. [3]. In this earlier research, a sufficient condition for stability and a control system design method were given. In this paper, we present a necessary and sufficient stability condition and develop an efficient method for computing the closed-loop stability for periodic, repetitive control systems. We propose design methods for linear, periodic, time-varying, repetitive control systems based on frozen-time system models and gain scheduling control [4].

The proposed control, as well as other design methods, are applied to the control of a fast machine-tool stage for the variable-speed machining, noncircular turning process (VSM-NCTP). In recent years, researchers have investigated the use of fast machine-tool stages for generating noncircular workpieces on a lathe and dynamic error compensation. As in any machining operation, chatter can adversely affect machining productivity by limiting the allowable depth of cut or feedrate. Chatter arises when the machine tool/workpiece structure and cutting process combine to form a dynamically unstable system. Machine tool structures have been made with high structural stiffness to combat this instability. However, in many situations, it is the low rigidity of the workpiece that is the cause of the cutting instability. One approach to increase the cutting stability margin in these situations is to apply variable-speed machining (VSM), which refers to machining operations in which the spindle speed is continuously varied in a periodic fashion over some nominal constant speed. To date, the use of VSM has been considered for passive machining operations only. The challenge that arises in controlling a fast machine-tool stage for VSM-NCTP is that the fast-tool stage is represented by a time-varying (discrete-time) system.

The remainder of this paper is organized as follows: First, problem formulation and previous research in periodic, repetitive control are given, and then a necessary and sufficient condition for closed-loop stability is derived. Periodic, repetitive control algorithms are then described and compared in simulation and experiment. Finally, experimental results of the fast-tool stage operating under VSM are presented.

2 Problem Formulation. The following notation will be adopted. G, $\bar{G}$, and $\tilde{G}$ (uppercase) represent systems and u, $\bar{u}$, and $\tilde{u}$ (lowercase) represent signals in the continuous-time, discrete-time and lifted domains, respectively. The discrete-time index, discrete-time delay operator, Laplace transform operator and z-transform operator are designated by k, q^{-1}, s, and z, respectively.

It will now be established that a continuous-time plant sampled

[1]Presently with Seagate Technologies, Inc.

Contributed by the Dynamic Systems and Control Division for publication in the JOURNAL OF DYNAMIC SYSTEMS, MEASUREMENT, AND CONTROL. Manuscript received by the Dynamic Systems and Control Division June 1, 1998. Associate Technical Editor: T. Kurfess.

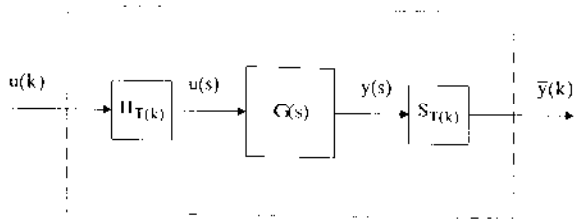

Fig. 1 Plant sampled at periodic rate

at a periodic rate can be represented by a periodic, discrete-time model. Consider the system shown in Fig. 1. In this figure, $G(s)$ represents the continuous-time plant model, and $S_{T(k)}$ and $H_{T(k)}$ represent a sampler and a zero-order hold, respectively. $S_{T(k)}$ and $H_{T(k)}$ operate at a synchronized, periodic, time-varying sampling rate, $T(k)$, having fixed period N, i.e.,

$$T(k+N)=T(k)\forall k. \tag{1}$$

Let the continuous-time, state-space representation for the plant be described in terms of (A_p,B_p,C_p,D_p). It is straightforward to show that the discrete-time equivalent plant can be expressed as

$$\bar{G}_p=\left[\begin{array}{cc}\bar{A}_p(k) & \bar{B}_p(k)\\ \bar{C}_p & \bar{D}_p\end{array}\right]=\left[\begin{array}{cc}e^{A_pT_k} & \left(\int_0^{T_k}e^{A_p t}dt\right)B_p\\ C_p & D_p\end{array}\right]. \tag{2}$$

It follows immediately from Eq. (1) that $\bar{G}_p$ represents a linear N-periodic discrete-time plant.

The repetitive control system considered in this paper is shown in Fig. 2. In this figure, $\bar{y}(k)$, $\bar{e}(k)$ and $\bar{y}_d(k)$ represent the closed-loop response, tracking error, and reference signal, respectively. Additionally, $\bar{G}_p$ represents the N-periodic discrete-time plant, and $\bar{G}_1$ and $\bar{G}_c$ comprise the time-varying, repetitive controller, which is restricted to be N-periodic. The role of $\bar{G}_1$ is to accumulate the tracking error over the period N to permit asymptotic tracking of N-periodic reference signals. The control system design objective consists of selecting the compensation filter $\bar{G}_c$ and design parameter L so that the resulting system is stable.

Repetitive control for linear, periodic systems has previously been studied by Omata et al. [3]. It is interesting to note that the motivation behind their research was to apply repetitive control to nonlinear systems, i.e., by linearizing a nonlinear plant about a periodic trajectory, a nonlinear plant could be represented by a linear periodic system.

The control system studied by Omata et al. is identical to that shown in Fig. 2. They showed that if the closed-loop system was stable, then $\bar{e}(k)\to 0$ as $k\to\infty$ for N-periodic inputs (asymptotic tracking). They also formulated a sufficient condition for stability. The stability condition, which was obtained using the small gain theorem, can be expressed as

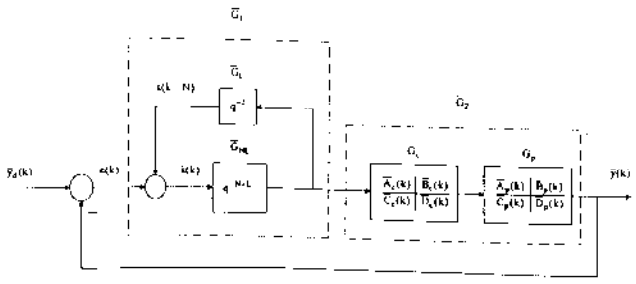

Fig. 2 Periodic repetitive control system

$$\|z^{-L}-\bar{G}_p\bar{G}_c\|_1<1 \tag{3}$$

where $\|\cdot\|_1$ represents the l_1 system norm. The left-hand side of this equation can be evaluated as

$$\|z^{-L}-\bar{G}_p\bar{G}_c\|_1=\sup_i\sum_{k=N}^{i}|\delta(i-k-L)-h(i,k)| \tag{4}$$

where $h(i,j)$ is the impulse response of $\bar{G}_p\bar{G}_c$ and δ is the ideal impulse function.

Equation (4) also served as the basis for their control system design method since it provides a stabilizing measure. Since it was difficult to derive the l_1-norm optimal solution directly, the control system design method consisted of determining a controller that minimized the evaluation function defined by

$$J=\max_{0<k<N}\sum_{l=0}^{M_0}|\delta(l-L)-h(k+l,k)|^2 \tag{5}$$

where M_0 is an appropriately large integer. The resulting controller has the form of a finite impulse response N-periodic filter.

3 Necessary and Sufficient Stability Condition

Let the state-space representation for blocks $\bar{G}_L$ and $\bar{G}_{NL}$ in Fig. 2 be expressed in terms of $(\bar{A}_L,\bar{B}_L,\bar{C}_L,0)$ and $(\bar{A}_{NL},\bar{B}_{NL},\bar{C}_{NL},0)$, respectively. Block $\bar{G}_1$ can then be expressed as

$$\bar{G}_1=\left[\begin{array}{c|c}\bar{A}_1 & \bar{B}_1\\ \hline \bar{C}_1 & 0\end{array}\right]=\left[\begin{array}{cc|c}\bar{A}_{NL} & \bar{B}_{NL}\bar{C}_L & \bar{B}_{NL}\\ \bar{B}_L\bar{C}_{NL} & \bar{A}_L & 0\\ \hline \bar{C}_{NL} & 0 & 0\end{array}\right] \tag{6}$$

In addition, block $\bar{G}_2$ can be described as

$$\bar{G}_2=\left[\begin{array}{c|c}\bar{A}_2(k) & \bar{B}_2(k)\\ \hline \bar{C}_2(k) & \bar{D}_2(k)\end{array}\right]=\left[\begin{array}{cc|c}\bar{A}_c(k) & 0 & \bar{B}_c(k)\\ \bar{B}_p(k)\bar{C}_c(k) & \bar{A}_p(k) & \bar{B}_p(k)\bar{D}_c(k)\\ \hline \bar{D}_p(k)\bar{C}_c(k) & \bar{C}_p(k) & \bar{D}_p(k)\bar{D}_c(k)\end{array}\right] \tag{7}$$

The state-space representation for the closed-loop system, $\bar{G}_{cl}$, may now be written as

$$\bar{G}_{cl}=\left[\begin{array}{c|c}\bar{A}_{cl}(k) & \bar{B}_{cl}(k)\\ \hline \bar{C}_{cl}(k) & \bar{D}_{cl}(k)\end{array}\right]=\left[\begin{array}{cc|c}\bar{A}_1-\bar{B}_1\bar{D}_2(k)\bar{C}_1 & -\bar{B}_1C_2(k) & \bar{B}_1\\ \bar{B}_2(k)\bar{C}_1 & \bar{A}_2(k) & 0\\ \hline \bar{D}_2(k)\bar{C}_1 & \bar{C}_2(k) & 0\end{array}\right] \tag{8}$$

The lifting technique is used to transform this N-periodic system into a higher dimensional LTI system $\tilde{G}_{cl}$. Some details of the lifting technique are given in the Appendix. For a more comprehensive description of the lifting technique, the reader is referred to Chen and Frances [5]. Since the lifting operation is norm preserving, the original periodic system is stable if and only if the transformed system is stable. The details of the lifting operation are omitted for brevity, but, by utilizing this technique, it is straightforward to show that a periodic, repetitive control system is stable if and only if

$$r(\tilde{A}_{cl})<1, \tag{9}$$

where

$$\tilde{A}_{cl}=\bar{A}_{cl}(N-1)\bar{A}_{cl}(N-2)\cdots\bar{A}_{cl}(0) \tag{10}$$

and $r(\cdot)$ is the spectral radius. The amount of computation represented by Eq. (10) is in the order of N^4 and is inefficient for large N (see Appendix). An alternative method for forming $\bar{A}_{cl}$ utilizing the N-delay operator in the repetitive controller requires computation in the order of N^3, significantly less for large N.

The control system design could also be performed in the lifted domain using standard MIMO design techniques. However, the resulting compensation filter $\bar{G}_c$ would have $N+n$ states (assuming a standard output-feedback design is used) where n is the number of states of the plant. Since N is typically large, this is not considered to be a practical approach.

4 Proposed Repetitive Control Algorithms

In this section, two control system design methods are presented which are based on the discrete-time, repetitive controller formulated by Tomizuka et al. [6]. The control system considered by Tomizuka et al. was identical to that shown in Fig. 2 except the plant was assumed to be time-invariant. To summarize the design procedure, let the transfer function for the plant be described as

$$\bar{G}_p(z^{-1}) = \frac{z^{-d}B(z^{-1})}{A(z^{-1})},$$

$$A(z^{-1}) = 1 - a_0 z^{-1} - \cdots - a_n z^{-n}, \text{ and}$$

$$B(z^{-1}) = b_0 + b_1 z^{-1} + \cdots + b_m z^{-m} \tag{11}$$

where d is the plant delay and is adjusted such that b_0 is nonzero. The compensation filter and design parameter L can be chosen as

$$\bar{G}_c(z^{-1}) = k_r \frac{A(z^{-1})(z^{-m}B(z))}{b} \tag{12}$$

(referred to as zero-phase error compensation) and

$$L = d + m \tag{13}$$

where $b = (|b_0| + |b_1| + \cdots + |b_m|)^2$ and $B(z)$ is obtained by substituting z for z^{-1} in $B(z^{-1})$. This controller is known to be stabilizing provided the repetitive controller gain k_r is in the range $0 < k_r < 2$. It is noted that, for brevity, the above is not a complete description of the repetitive control system design proposed by Tomizuka et al. (no distinction made between stable and unstable zeros in this discussion).

Control System Design Based on the Nominal Model. A LTI controller described by Eqs. (12) and (13) based on the nominal plant model was designed. Intuitively, one would expect this method to result in a stabilizing controller if the variation in plant dynamics is small, but not if there are large variations. This is precisely the result observed in the case study given in this research. For situations in which this method results in a stabilizing controller, the resulting controller has the obvious advantage that it is LTI and hence easier and less costly to implement than the other methods described.

Control System Design Utilizing Gain Scheduling. To allow for a larger variation in the sample rate, gain scheduling, which is commonly used in nonlinear control system design, is suggested. Consider computing the nominal models for the plant over small time segments, and then designing a controller as described by Eqs. (12) and (13) for each of these segments. By implementing the controller so that the gains are scheduled accordingly, a larger variation in the plant dynamics may be permissible. In general, it would be expected that decreasing the size of the time segments would increase the likelihood of obtaining a stabilizing controller. The limiting case would be to perform N controller designs given an N-periodic controller. This is the suggested design method of this section.

This design method is summarized as follows: Form the discrete-time equivalent of the plant $\bar{G}_p(z^{-1}, k)$ at each k ranging from 0 to $N-1$. Compute the coefficients for the compensation filter of Eq. (12) for each k. The resulting N sets of coefficients represent the N-periodic coefficients of the desired controller. L is set equal to the constant $d+m$. The closed-loop stability must be assessed by (9) after the design is complete since the resulting controller is not necessarily stabilizing.

Modified Periodic Repetitive Control System. For LTI repetitive control systems, a low-pass Q-filter is often inserted in the repetitive signal generator (internal model) to achieve robust stability (Tsao and Tomizuka [7]). The low-pass filter is placed in series with block $\bar{G}_{NL}$ in Fig. 2, i.e., replacing q^{-N+L} with $Q(k,q,q^{-1})q^{-N+L}$ in Fig. 2. A Q-filter can be incorporated into the periodic repetitive control system in the same fashion as the time-invariant counterpart. For the periodic repetitive case, the Q-filter, $Q(k,q,q^{-1})$, is allowed to be noncausal and periodically time-varying. For the modified system, the spectral radius of Eq. (9) can be computed as before except that $(A_{NL}, B_{NL}, C_{NL}, 0)$ is replaced with the state space representation for $Q(k,q,q^{-1})q^{-N+L}$. The price for the increase in relative stability is a decrease in tracking performance at high frequencies. It is noted that for the case of an LTI system, a stability condition, based on quantified unmodeled dynamics, can be derived (Tsao and Tomizuka [7]). For the case of a periodically varying system, a general stability condition is not presently known. However, it is shown in the following sections that the inclusion of a Q-filter does increase the stability margin for the problem at hand.

5 Application to the Control of a Fast Machine-Tool Stage for VSM-NCTP

In this section, the control of a fast machine-tool stage for VSM-NCTP is considered and the performance obtained using each of the control design methods described above are compared both theoretically and experimentally. This section begins by giving a brief background in VSM. Then, the theoretical and experimental performance obtained using the various design methods is compared. Finally, experimental machining results are given.

Background in Variable Speed Machining. Stoferle and Grab [8] introduced the VSM concept for improving the cutting stability in single point machining operations. Since that time, numerous studies have been conducted addressing various topics in VSM. Hoshi et al. [9] experimentally demonstrated the effectiveness of VSM for improving the cutting stability in turning and boring operations. Analog simulations were performed by Sexton and Stone [10,11] to predict the effects of VSM on the stability charts in single point operations. Theoretical analysis has been performed by Inamuara and Sata [12] and Tsao et al. [13] to predict the cutting stability of VSM operations. Several studies have also been conducted addressing the use of VSM for interrupted machining operations (Lin [14], Englehart et al. [15]).

An important issue in these previous studies has been the choice of the spindle speed trajectory. For practical reasons, it has been suggested that the spindle speed trajectory be a single sine wave described by (Lin [16], Englehart et al. [15])

$$\omega(t) = \omega_0 + A\sin(2\pi f t) \tag{14}$$

where ω_0 is the nominal spindle speed, A is the amplitude of the variation in speed, and f is the frequency of the speed variation. A nondimensional expression describing this speed trajectory can be expressed as (Lin [14])

$$\omega(t) = \omega_0[1 + \mathrm{RVA}\sin(\mathrm{RVF}\,\omega_0 t)] \tag{15}$$

where $\mathrm{RVA} = A/\omega_0$ represents the relative amplitude of the trajectory and $\mathrm{RVF} = 2\pi f/\omega_0$ represents the relative frequency of the trajectory.

The general finding in the previous research is that increasing the values of RVF or RVA typically results in a reduction of the chatter level or, in other words, results in an increase in the machining stability margin. The values of RVA and RVF that can be

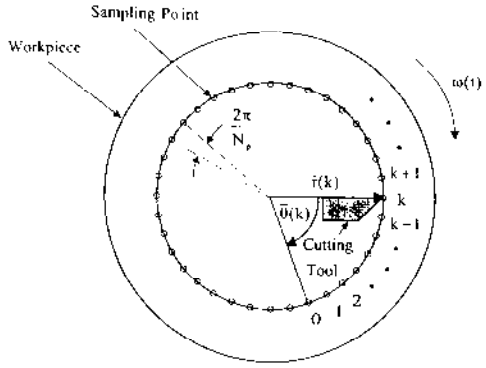

Fig. 3 Sampling scheme for VDCM/VSM operation

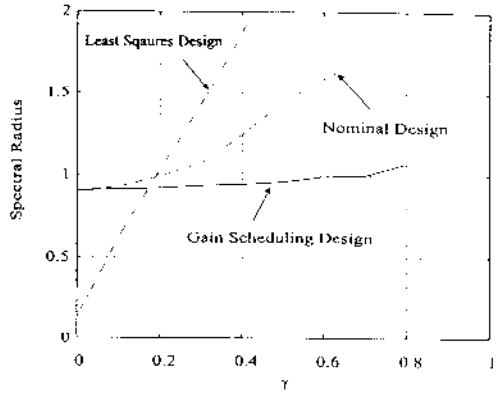

Fig. 4 Comparison of design methods

practically implemented typically range from 0.1 to 0.3 and are limited by motor performance and capacity envelope (Lin [14]).

Proposed Method to Control a Fast Machine-Tool Stage Operating Under VSM. The proposed method to control a fast machine-tool stage for VSM-NCTP is to control the sampling rate and spindle speed such that both the reference signal and plant become periodic with the same period N. By doing so, periodic repetitive control can be utilized to control the fast machine-tool stage.

The reference and plant are made N-periodic by the following conditions:

(i) The sampling occurs at a fixed angular interval which integrally divides one spindle rotation.
(ii) The spindle speed trajectory is periodic in the angular domain, and the period of the spindle speed trajectory is an integral multiple of spindle rotations.

The situation described by conditions (i) and (ii) is depicted in Fig. 3 for a boring operation in which the workpiece rotates. The profile of the workpiece is described in terms of the coordinates r and θ. In this figure, the workpiece is shown rotating at a periodic spindle trajectory ω. The sampling instances are triggered at N_p points around the circumference of the workpiece.

Comparison of Design Methods based on Theoretical and Experimental Results. The fast machine-tool stage used for the VSM-NCTP experiment is a piezoelectric actuated boring bar, which has been used to compensate for cutting-force-induced bore cylindricity errors (Hanson and Tsao [16–18]). The dynamic model is

$$G(s)=\frac{b_0}{s^4+a_3s^3+a_2s^2+a_1s+a_0}\cdot\frac{1}{ms^2+cs+k} \tag{16}$$

where

$$\{b_0,a_0,a_1,a_2,a_3,m,c,k\}=\{3.34e18,2.18e18,3.30e14,\ 1.04e10,1.79e5,0.365,208,12.8e6\}. \tag{17}$$

and the periodic sample rate considered is

$$T(k)=T_{\text{nom}}+\gamma T_{\text{nom}}\sin(2\pi k/N). \tag{18}$$

The sampling rate described Eq. (18) is analogues to the sampling rate occurring under VSM where the spindle trajectory is described by Eq. (15).

As discussed in the background section for VSM, it is desirable for spindle speed trajectory to operate over a wide range of RVA or equivalently γ. Therefore, the range of γ over which stabilizing controllers are obtained for the various control design methods are compared below both theoretically and experimentally.

The three control design methods previously mentioned are compared. Controllers were designed using each of these three methods over a range of γ, and the corresponding spectral radii of Eq. (10) were computed. The results are shown in Fig. 4. In this figure, the design method given in Section 2 is labeled "Least Squares Design," the nominal plant design of Section 5 is labeled "LTI Zero Phase," and the gain scheduling approach of Section 5 is labeled "PTV Zero Phase." The gain scheduling design yielded the maximum range of γ (up to 0.7) over which stabilizing controllers were obtained. The other two methods yielded stabilizing controllers for γ up to approximately 0.2. In this analysis, the values used for T_{nom}, N, and k_r in this example are 250 μs, 32, and 1, respectively, and the filter Q is unity.

In the Least Squares design method using the l_1 formulation, the design parameter L was set equal to 3 since this was determined to yield the largest stable range. The resulting controller had 12 periodic coefficients. This compares to 12 constant coefficients for the nominal plant design and 12 periodic coefficients for the gain scheduling design approach.

The values used for N in the above examples were kept relatively small to limit the amount of computation. It is interesting to note that N has relatively little effect on the spectral radius in the examples considered. For example, Fig. 5 shows the effect of N on the spectral radius for designs using the gain-scheduling controller. In generating the plot, the value used for γ was 0.3, and N ranged from 32 to 1000.

In this experiment, the boring bar servo system was operated with a periodically varying sampling rate as described by Eq. (18). Repetitive controllers were implemented over a range of γ using each of the three design approaches. The objective of this experiment was to determine the range of γ over which stable implementations were observed.

For each of the design methods, γ was initially set to 0.1 and then increased in increments of 0.1 until an unstable system was

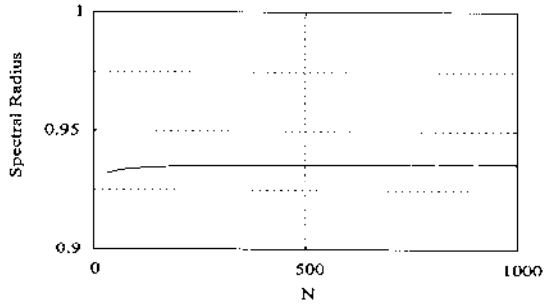

Fig. 5 Effect of increasing N on spectral radius computation

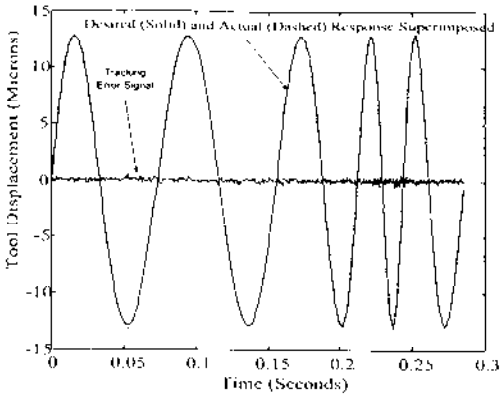

Fig. 6 Example of tracking results obtained

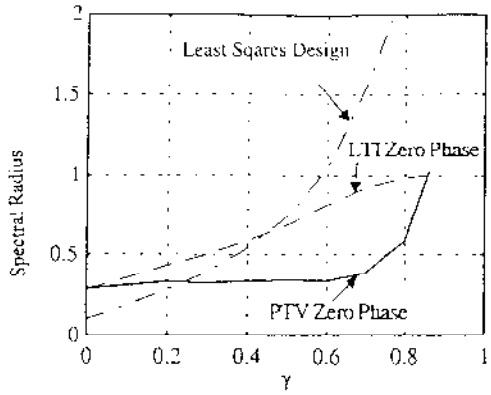

Fig. 7 Stabilizing effect of Q filter

experimentally observed. In this experiment, the nominal sampling rate was 250 μs and N was 1200. Also, the reference signal utilized was

$$\bar{y}_d(k) = \text{AMP} \cdot \sin\left(\frac{2\pi\eta}{N}k\right) \tag{19}$$

where AMP and η were 12.5 microns and 5, respectively.

It was observed that when using the l_1 formulation, the implementation was stable for γ equal to 0.1 but was unstable for γ equal to 0.2. Similarly, when the design procedure based on the nominal-plant model was used, the resulting system was stable for γ equal to 0.1 but was unstable for γ equal to 0.2. The gain scheduling design approach resulted in stable systems for γ ranging from 0.1 to 0.5, but resulted in an unstable system for γ equal to 0.6. To serve as an example of the tracking performance obtained in these experiments, results obtained for the gain scheduling design operating with a γ of 0.5 are shown in Fig. 6. This plot shows the reference signal and the actual response superimposed as well as an additional curve representing the tracking error signal.

Table 1 summarizes the results of this experiment. Note that the range of γ over which stable designs were obtained experimentally agrees with the theoretical predictions given in Fig. 4. Also listed in Table 1 are the root-mean-square (RMS) values of the tracking error computed for each stable design obtained.

When implementing each of the controllers represented in Table 1, a Q-filter described by

$$Q(z,z^{-1}) = 0.1z + 0.8 + 0.1z^{-1} \tag{20}$$

was included in the control implementation to account for unmodeled dynamics. In this experiment, it was observed that if the Q-filter was not included in the controller implementation, none of the systems represented in Table 1 operated stably.

The stabilizing effect of the Q filter for the present periodic control systems is further illustrated by Fig. 7, where the spectral radius were computed with the following Q filter inserted to the controllers described above:

$$Q(z,z^{-1}) = 0.25z + 0.5 + 0.25z^{-1} \tag{21}$$

The range of γ for which a stabilizing controller is obtained is significantly increased for each of the three controllers.

Experimental Machining Results. In this experiment, 6 workpieces were bored using a two-pass machining operation. The geometry of the cutting tool used in this experiment was a lead angle of 5 deg, a radial rake angle of 0 deg, an axial rake angle of 5 deg, and a nose radius of 4.76 mm. The workpieces are 12.7 mm long schedule 80 steel pipe mounted in a three-jaw chuck. In the first pass, the cutting tool mounted on the rigid side of the boring bar was used to reduce the bore wall thickness to approximately 3.2 mm. In the second pass, the cutting tool was mounted on the variable depth of cut side of the boring bar and used to machine an elliptical bore profile (i.e., $\eta = 10$, $N = 1200$ in (19)) with a peak to peak amplitude of 46 μm. During the second pass, the nominal depth of cut, spindle speed, and feed rate were 0.764 mm, 1000 rpm, and 0.1 mm/rev, respectively. These cutting conditions were selected since it was found through trial that they resulted in a small level of chatter for the case of constant speed machining. Three workpieces were machined using a constant spindle speed in the second pass. The remaining three workpieces were machined under a variable speed operation in which the values for RVA and RVF were both 0.2.

The tracking error was recorded for duration of 15 spindle rotations during the second pass. These measurements were recorded when the cutting tool had passed 1 mm into the workpiece in the feed direction. From these data the RMS value of the tracking error was computed for each test and is listed in Table 2. Note that the VSM operation consistently reduced the vibration level over the constant spindle speed operation. The results obtained in two of these tests are also shown in Figs. 8 and 9 for comparison.

The digital controller implemented in this experiment was the gain scheduling design. Note from Table 1, that for the value of 0.2 used for RVA (or equivalently γ), only the gain scheduling method resulted in a stabilizing design.

Table 1 Experimental comparison of design methods

γ	0.1 (microns)	0.2	0.3	0.4	0.5	0.6
l_1 Formulation	stable 0.156 rms	**unstable**	X	X	X	X
Nominal Design	stable 0.156 rms	**unstable**	X	X	X	X
Gain Scheduling	stable 0.152 rms	stable 0.152 rms.	stable 0.151 rms.	stable 0.154 rms.	stable 0.169 rms.	**unstable**

Table 2 Comparison of constant speed and variable speed machining test results

Test #	Test Type	RMS Tracking Error (μm)
1	constant speed	3.9925
2	constant speed	2.0248
3	constant speed	2.9929
4	variable speed	0.7682
5	variable speed	0.6976
6	variable speed	0.7734

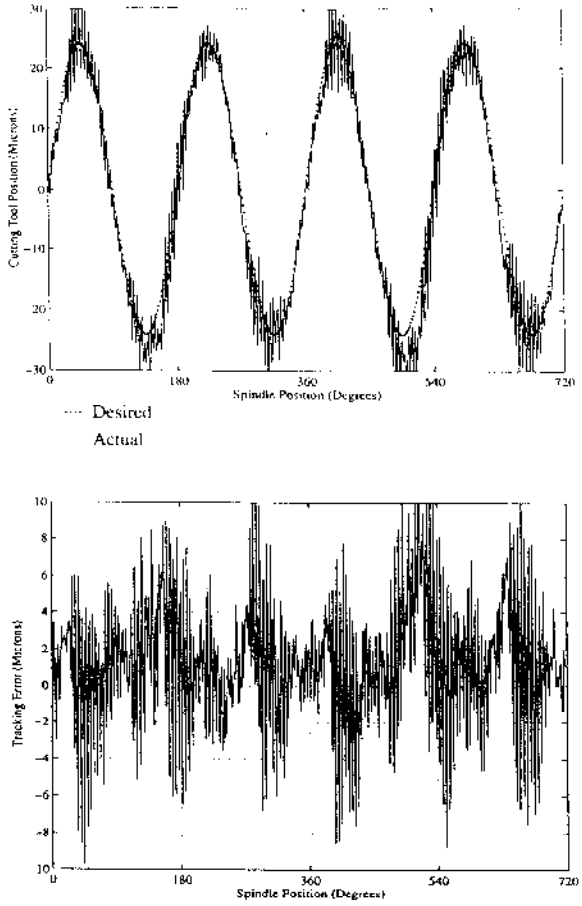

Fig. 8 Tracking performance under constant spindle speed-Test 1

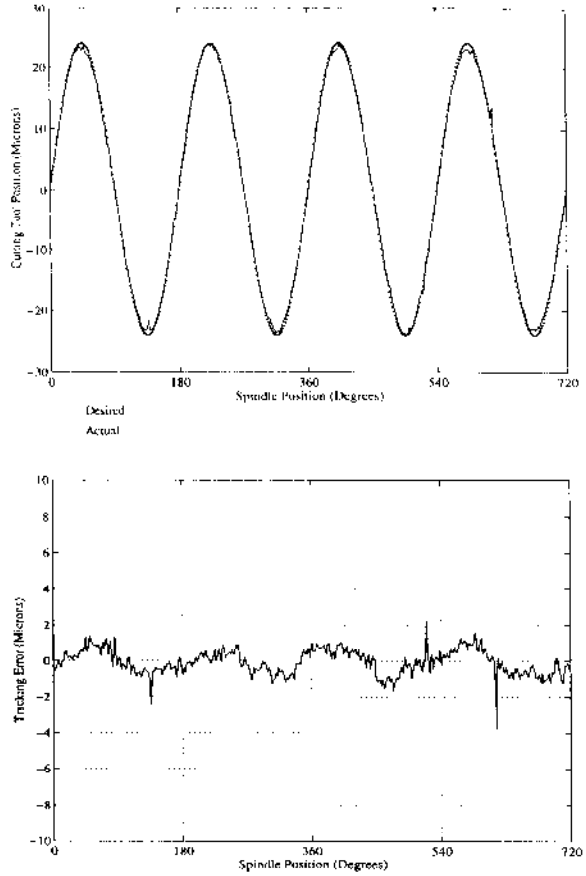

Fig. 9 Tracking performance under variable spindle speed-Test 4

6 Conclusions

Repetitive control for SISO LTI systems sampled at a periodic rate have been addressed. A necessary and sufficient stability condition and an efficient computation method that utilizes the special repetitive control structure have been developed for the periodic, repetitive control systems. The time-invariant, repetitive controller based on a nominal sampling interval is the easiest and least costly to implement. The gain scheduled, periodic, repetitive control yielded stabilizing controllers when the other methods failed for the cited variable speed machining application. The control methods have been applied to variable spindle speed, noncircular turning/boring by using a fast piezoelectric machine-tool stage. Significant reduction of the chatter vibration level has been observed when compared to that using constant speed machining.

Appendix

An Efficient Method for Computing $\bar{A}_{cl}$ for a Periodic Repetitive Control System. One approach for computing the lifted closed-loop system matrix, $\bar{A}_{cl}$, for a periodic, repetitive control system is by means of Eqs. (9) and (10). To evaluate Eq. (10), it is necessary to compute the product of N matrices, each having dimension $(N+n+m)$ by $(N+n+m)$ where N, n and m are the period of the plant, order of the plant and order of the controller, respectively. For large N, this represents a significant amount of computation including $N(N+n+m)^3$ multiplications (the product of two $N+n+m$ matrices requires $(N+n+m)^3$ multiplications and Eq. (10) represents the product of N matrices each having dimension $(N+n+m)$). In this section, a new approach for computing $\bar{A}_{cl}$ is given which is less computationally intensive.

The savings in computation result from the means in which the lifted representation for the closed-loop system is obtained. In the first approach, the closed-loop system is first formed and then a general expression for the lift of a periodic system is utilized (represented by Eqs. (A1) though (A7)). In the proposed approach, the individual blocks $\bar{G}_1$ and $\bar{G}_2$ in Fig. 2 are first lifted and then the governing equation for the closed-loop system is formed. The portion of the system that contains N states, namely the repetitive signal generator, is simple in form and can be lifted algebraically, as opposed to using the general expression, resulting in a large reduction in computation.

To develop the expressions for this second method, we start from Eq. (7). The lift of $\bar{G}_2$ over the base period N can be expressed as (Chen and Frances [5])

$$\bar{x}(i+1)=\bar{A}_2\bar{x}(i)+\bar{B}_2\bar{u}(i) \tag{A1}$$

$$\bar{e}(i)=-\bar{C}_2\bar{x}(i)-\bar{D}_2\bar{u}(i) \tag{A2}$$

where

$$\bar{A}_2=\Phi_2(N,N) \tag{A3}$$

$$\bar{B}_2=[\Phi_2(N,N-1)\bar{B}_2(0),\Phi_2(N,N-2)\bar{B}_2(1),\cdots \Phi_2(N,2)\bar{B}_2(N-3),\Phi_2(N,1)\bar{B}_2(N-2),\bar{B}_2(N-1)] \tag{A4}$$

$$\bar{C}_2=\begin{bmatrix}\bar{C}(0)\\ \bar{C}_2(1)\Phi_2(1,1)\\ \vdots\\ \bar{C}_2(N-1)\Phi_2(N-1,N-1)\end{bmatrix} \tag{A5}$$

$$\bar{D}_2=\begin{bmatrix} \bar{D}_2(0) & 0 & \cdots & & & 0 \\ \bar{C}_2(1)\bar{B}_2(0) & \bar{D}_2(1) & 0 & \cdots & & 0 \\ \bar{C}_2(2)\Phi_2(2,1)\bar{B}_2(0) & \bar{C}_2(2)\bar{B}_2(1) & \bar{D}_2(2) & 0 & \cdots & 0 \\ \bar{C}_2(3)\Phi_2(3,2)\bar{B}_2(0) & \bar{C}_2(3)\Phi_2(3,1)\bar{B}_2(1) & \bar{C}_2(3)\bar{B}_2(2) & \bar{D}_2(3) & 0 & 0 \\ \vdots & \vdots & & & & \vdots \\ \bar{C}_2(N-1)\Phi_2(N-1,N-2)\bar{B}_2(0) & \bar{C}_2(N-1)\Phi_2(N-1,N-3)\bar{B}_2(1) & \cdots & & & \bar{D}_2(N-1) \end{bmatrix} \quad (A6)$$

$$\Phi_2(k,j)=\bar{A}_2(k-1)\bar{A}_2(k-2)\cdots\bar{A}_2(k-j). \quad (A7)$$

For convenience, rearrange the repetitive signal generator, $\bar{G}_1$, of Fig. 2 as shown in Fig. A1, and define signals $e(k)$, $z(k)$, and $u(k)$ as shown in this figure. Note from Fig. A1 that

$$z(k)=e(k+L) \quad (A8)$$

and

$$u(k)=u(k-N)+z(k-N). \quad (A9)$$

From the definition of the lifting operation, it is easy to show that the lift of $\bar{G}_1$ can be expressed as

$$\bar{z}(i)=S^L\bar{e}(i)+D^{N-L}\bar{e}(i+1) \quad (A10)$$

and

$$\bar{u}(i)=\bar{u}(i-1)+\bar{z}(i-1) \quad (A11)$$

where S, D, and K are $N\times N$ matrices having the form

$$S=\begin{bmatrix} 0 & 1 & 0 & \cdots & 0 \\ 0 & 0 & 1 & & 0 \\ 0 & 0 & 0 & \ddots & 0 \\ \vdots & \vdots & \vdots & & 1 \\ 0 & 0 & 0 & \cdots & 0 \end{bmatrix} \quad (A12)$$

and

$$D=\begin{bmatrix} 0 & 0 & 0 & \cdots & 0 \\ 1 & 0 & 0 & & 0 \\ 0 & 1 & 0 & & 0 \\ \vdots & & \ddots & & \vdots \\ 0 & 0 & \cdots & 1 & 0 \end{bmatrix} \quad (A13)$$

The resulting expressions describing the closed-loop system matrix, $\bar{A}_{cl}$, obtained by combining Eqs. (A1), (A2), (A10), and (A11) are

$$\bar{A}_{cl}=\begin{bmatrix} \tilde{A} & \bar{B} \\ M_1 & M_2 \end{bmatrix} \quad (A14)$$

where

$$M_1=-(I+D^{N-L}\tilde{D})^{-1}[S^L\tilde{C}_2+D^{N-L}\bar{C}_2\tilde{A}_2] \quad (A15)$$

and

$$M_2=(I+D^{N-L}\bar{D})^{-1}[I-S^L\bar{D}_2-D^{N-L}\bar{C}_2\bar{B}_2] \quad (A16)$$

Note that the maximum number of multiplications required in forming any term involving $\Phi_2(k,j)$ in $\tilde{A}_2$, $\bar{B}_2$, $\bar{C}_2$, and $\bar{D}_2$ is $N(n+m)^3$, i.e., the worst case would be when k and i were both N, requiring the computation of the product of N matrices of dimension $n+m$. Therefore, forming $\tilde{A}_2$, $\bar{B}_2$, $\bar{C}_2$, and $\bar{D}_2$ requires at most $N(n+m)^3$, $N^2(n+m)^3$, $N^2(n+m)^3$ and $1/2N^3(n+m)^3$ (the 1/2 factor applies since $\bar{D}_2$ is lower triangular), respectively. Further, note that S^L and D^{N-L} can be formed by shifting the diagonal of ones and the matrix multiplication indicated need not be explicitly performed. The matrix $(I+D^{N-L}\bar{D})$ involved in Eqs. (A15) and (A16) is lower diagonal and its inverse can be computed efficiently. From the above discussion it can be seen that for large N this alternative approach represents significantly less computation than that of Eq. (10) requiring $N(N+n+m)^3$ multiplications.

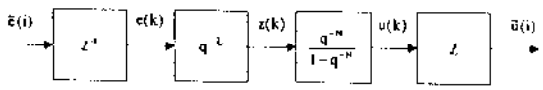

Fig. A1 Lifted repetitive signal generator

References

[1] Tsao, T.-C., and Pong, K. C., 1991, "Control of Radial Runout in Multi-Tooth Face Milling," Transactions of the North American Manufacturing Research Institute of SME, pp. 183–190.

[2] Tsao, T.-C., and Pong, K. C., 1992, "Spindle Speed Regulation and Tracking in Interrupted Cutting," Transactions of the North American Manufacturing Research Institute of SME, pp. 235–241.

[3] Omata, T., Hara, T., and Nakano, M., 1985, "Repetitive Control for Linear Periodic Systems," Electr. Eng. Jpn., **105**, pp. 133–139.

[4] Hanson, R. D., and Tsao, T.-C., 1996, "Discrete-Time Repetitive Control of LTI Systems Sampled at a Periodic Rate," Proc. of IFAC'96 World Congress, Vol. D 13-18, San Fransisco.

[5] Chen, T., and Francis, B., 1995, Sampled-Data Control Systems, Chap. 8, Springer-Verlag, England.

[6] Tomizuka, M., Tsao, T.-C., and Chew, K.-K., 1989, "Analysis and Synthesis of Discrete-Time Repetitive Controllers," ASME J. Dyn. Syst., Meas., Control, **111**, pp. 353–358.

[7] Tsao, T.-C., and Tomizuka, M., 1994, "Robust Adaptive and Repetitive Digital Tracking Control and Application to Hydraulic Servo for Noncircular Machining," ASME J. Dyn. Syst., Meas., Control, **116**, pp. 24–32.

[8] Stoferle, T., and Grab, H., 1972, "Vermeiden von Ratterschwingungen durch periodische Drehzahlanderung," Werkstatt und Betrieb, **105**, pp. 727–731.

[9] Hoshi, T., Sakisaka, N., Moriyama, T., and Sato, M., 1977, "Study for Practical Application of Fluctuating Speed Cutting for Regenerative Chatter Control," Ann. CIRP, **25**, pp. 175–179.

[10] Sexton, J., and Stone, B., 1980, "Investigation of the Transient Effects during Variable Speed Machining," J. Mech. Eng. Sci., **22**, pp. 107–110.

[11] Sexton, J., and Stone, B., 1978, "The Stability of Machining with Continuously Varying Spindle Speed," Ann. CIRP, **107**, pp. 321–323.

[12] Inamura, T., and Sata, T., 1974, "Stability Analysis of Cutting Under Varying Spindle Speed," Ann CIRP, **23**, pp. 119–123.

[13] Tsao, T.-C., McCarthy, M., and Kapoor, S., 1993, "A New Approach to Stability Analysis of Variable Speed Machining Systems," Int. J. Machine Tools & Manufacture, **33**, No. 6, pp. 791–808.

[14] Lin, S.-C., 1989, "The Use of Variable Spindle Speed for Vibration Control In Face Milling Process," Ph.D. thesis, University of Illinois at Urbana-Champaign.

[15] Englehart, R., Lin, S., DeVor, R., and Kapoor, S., 1989, "A Verification of the Use of Variable Spindle Speed for Vibration Reduction in Face Milling," *Proceedings of the 17th North American Manufacturing Research Conference*, pp. 115–121.

[16] Hanson, R. D., and Tsao, T.-C., 1994, "Development of a Fast Tool Servo for Variable Depth of Cut Machining," *Proc. ASME Winter Annual Meeting-Dynamic Systems and Control*, **2**, pp. 863–871.

[17] Hanson, R. D., and Tsao, T.-C., 1996, "Compensation for Cutting Force Induced Bore Cylindricity Dynamic Errors–A Hybrid Repetitive Servo/Iterative Learning Process Feedback Control Approach," *Japan USA Symposium on Flexible Automation*, Boston, MA, pp. 1019–1026.

[18] Hanson, R. D., and Tsao, T.-C., 1998, "Reducing Cutting Force Induced Bore Cylindricity Errors by Learning Control and Variable Depth of Cut Machining," ASME J. Manuf. Sci. Eng., **120**, pp. 547–554.